Published August 15, 1991

A Potential Role for the COOH-terminal Domain in the Lateral Packing of Type III Intermediate Filaments

Panos D. Kouklis, Thomais Papamarcaki, Andreas Merdes, and Spyros D. Georgatos

Programme of Cell Biology, European Molecular Biology Laboratory, Meyerhofstrasse 1, 6900 Heidelberg, Germany

Abstract. To identify sites of self-association in type III intermediate filament (IF) proteins, we have taken an "anti-idiotypic antibody" approach. A mAb (anti-Ct), recognizing a similar feature near the end of the rod domain of vimentin, desmin, and peripherin (epsilon site or epsilon epitope), was characterized. Anti-idiotypic antibodies, generated by immunizing rabbits with purified anti-Ct, recognize a site (presumably "complementary" to the epsilon epitope) common among vimentin, desmin, and peripherin (beta site or beta epitope). The beta epitope is represented in a synthetic peptide (PII) modeled after the 30 COOH-terminal residues of peripherin, as seen by comparative immunoblotting assays. Consistent with the idea of an association between the epsilon and the beta site, PII binds in vitro to intact IF proteins and fragments containing the epsilon epitope, but not to IF proteins that do not react with anti-Ct. Microinjection experiments conducted in vivo and filament reconstitution assays carried out in vitro further demonstrate that "uncoupling" of this site-specific association (by competition with PII or anti-Ct) interferes with normal IF architecture, resulting in the formation of filaments and filament bundles with diameters much greater than that of the normal IFs. These thick fibers are very similar to the ones observed previously when a derivative of desmin missing 27 COOH-terminal residues was assembled in vitro (Kaufmann, E., K. Weber, and N. Geisler. 1985. *J. Mol. Biol.* 185:733-742). As a molecular explanation, we propose here that the epsilon and the beta sites of type III IF proteins are "complementary" and associate during filament assembly. As a result of this association, we further postulate the formation of a surface-exposed "loop" or "hairpin" structure that may sterically prevent inappropriate filament-filament aggregation and regulate filament thickness.

INTERMEDIATE filaments (IFs)[1] constitute conspicuous components of the eukaryotic cytoplasm (Lazarides, 1980; Steinert and Roop, 1988). These elements consist of protein subunits organized in (at least) two supramolecular levels: the level of the filament, where subunits self-associate in a specific manner to produce a linear 10-nm "rope" structure, and the level of the filament network, where arrays of IFs integrate into higher order formations and associate with other organelles. Typical 10-nm filaments can be reconstituted in vitro from isolated subunits (Renner et al., 1981; Zackroff and Goldman, 1979). However, IF network assembly in vivo apparently involves multiple heterotypic interactions between IF subunits and other cellular factors.

IF proteins are chemically heterogeneous and can be classified in five distinct categories (Steinert and Roop, 1988). Type I and II subunits include the cytokeratins, type III proteins include the subunits vimentin, desmin, peripherin, and GFAP, type IV subunits comprise the neurofilament triplet proteins, and type V subunits are represented by the nuclear lamins. Despite their heterogeneity, all of these proteins possess a similar domain substructure, consisting of an alpha-helical middle domain ("rod") and two nonhelical end domains ("head" and "tail"). Whereas the helical domain is highly conserved among different subunit species, the nonhelical domains vary in sequence and sequence principles (Hanukoglu and Fuchs, 1983; Geisler and Weber, 1982; Geisler et al., 1982).

The structural role of the middle domain has been explored in previous studies both in vitro (Geisler et al., 1982) and in vivo (Albers and Fuchs, 1987, 1989). By consensus, this domain is thought to be responsible for the initial aggregation of IF chains into coiled-coil dimers from which higher oligomers arise (see also Coulombe and Fuchs, 1990). However, the involvement of the end domains in filament formation remains unclear. On one hand, ultrastructural data suggest that these segments are not integral parts of the IF core, but rather peripheral elements protruding from the filament proper (Geisler et al., 1982; Hisanaga and Hirokawa, 1988; Steinert et al., 1983; Steven et al., 1989). On the other

Dr. Papamarcaki's present address is Laboratory of Biological Chemistry, Medical School, University of Ioannina, Ioannina, Greece.

1. *Abbreviations used in this paper*: IF, intermediate filament; NF-L, intact neurofilament L protein.

Published August 15, 1991

hand, several studies indicate that the NH_2-terminal domain is essential for IF assembly in vitro (Kaufmann et al., 1985; Traub and Vorgias, 1983) and, in some cases, that both of the end domains are required for normal IF assembly in vivo (Gill et al., 1990; Lu and Lane, 1990). Other studies further underscore the potential significance of the end domains, suggesting that they may be involved in the organization of IF networks via specific interactions with components of the nuclear envelope and the plasma membrane (Djabali et al., 1991; Georgatos and Blobel, 1987*a*,*b*; Georgatos et al., 1987).

To better understand the role of the end domains in filament assembly, we have designed a new scheme of analysis based on the ability of network (idiotypic/anti-idiotypic) antibodies to recognize "complementary" interacting sites in molecules that associate with each other. In principle, this method involves production of (secondary) antibodies using as an antigen (primary) mAbs against specific determinants of the end domains of IF subunit molecules. By convention (Jerne, 1974, 1985), those secondary antibodies that (*a*) would bind specifically to the antigen-binding sites of the primary antibodies; and (*b*) would react with IF subunits of the same class, are expected to recognize epitopes "stereo-complementary" to the epitopes recognized by the primary antibodies. Thus, each idiotypic/anti-idiotypic antibody pair defines a potential interaction between two different sites along IF protein chains. Whether or not such an interaction occurs under physiological conditions can be examined in a second step using independent biochemical methods and in vivo analysis.

Materials and Methods

Protein Chemical Procedures

Rat liver lamin B was isolated as reported by Georgatos and Blobel (1987*b*). Mouse vimentin was purified from tissue culture cells (Nelson and Traub, 1982). Other intermediate filament proteins and their proteolytic derivatives were prepared as previously described (Geisler et al., 1982; Georgatos et al., 1987*a*,*b*; Kaufmann et al., 1985). Purified desmin rod fragments and intact neurofilament L protein (NF-L) subunits were kindly provided by N. Geisler and K. Weber (Max-Planck Institute for Biophysical Chemistry, Goettingen, Germany). Synthetic peptides (PI, PII and DI, see Djabali et al., 1991; Georgatos et al., 1987) were made at Rockefeller University Biopolymer Facility (New York, NY), according to the published cDNA sequences coding for rat peripherin (Leonard et al., 1988; Landon et al., 1989) and chicken desmin (Geisler and Weber, 1982). To prepare protofilamentous forms of vimentin, the purified protein was dialyzed from a 6 M urea, 10 mM Tris-HCl, pH 7.0 buffer into a solution of 5 mM Tris-HCl, pH 7.4. The absence of filaments and the existence of protofilamentous species was assessed by EM. Filament formation was initiated by adjustment of the salt (KCl) to 150 and 10 mM Tris-HCl by dilution of concentrated samples into the assembly buffer. Affinity columns were made by coupling PII to derivatized agarose (Affigel-15) as specified in Georgatos and Blobel (1987*b*).

Assays

Ligand-blotting assays were performed as described previously (Georgatos et al., 1987). Dot-blots were done as described by Djabali et al. (1991).

Immunological and Immunochemical Procedures

Anti-Ct mAbs were prepared using as an antigen the fusion protein 399 (containing 100 COOH-terminal residues of mouse vimentin and 99 NH_2-terminal residues of MS2-RNA polymerase). For details about the construction of 399 and immunization see Kouklis (1990). To generate anti-idiotypic antibodies, the EMBL standard protocol was followed. Purified anti-Ct IgG was injected in the thigh lymph nodes and subcutaneously in rabbits (200 μg per animal, in complete Freunds adjuvant) at day 0. After boosting at day 21 (200 μg, in incomplete Freunds adjuvant, subscupularly), sera were collected after 1 wk. Immunization continued for another 12 wk (weekly injections of 200 μg anti-Ct, intramuscularly) and blood was collected every week. Comparative immunoblotting showed that the anti-idiotypic activity peaked in the second bleed. Affinity chromatography (isolation of antibodies by a PII-affigel-15 column) was performed as follows: 3 ml of #28 immune serum, reconstituted with 0.1% Tween-20, was incubated batchwise with Affigel 15-PII (~7.5 mg PII/ml) for 1 h at room temperature. The slurry was packaged into a column, and washed with 20 ml of isotonic buffered saline containing 0.1% Tween-20 (washing buffer) followed by 20 ml of PBS. The bound antibodies were eluted with 15 ml of 200 mM glycine-HCl, pH 2.3, 500 mM NaCl in tubes containing 500 mM Na_2HPO_4. Eluted antibodies were extensively dialyzed at 4°C against washing buffer. Fab fragments were isolated from anti-Ct IgG using papain beads and protein G-affinity chromatography (Pierce Handbook and General Catalogue, 1989, Pierce, Europe).

Immunoblotting was performed as previously described (Georgatos and Blobel, 1987*b*). For immunofluorescence microscopy, 3T3 cells were fixed for 10 min in 4% paraformaldehyde in PBS, pH 7.2. After quenching with 50 mM NH_4Cl, the cells were extracted for 10 min with 0.5% Triton X-100. Vimentin intermediate filaments were stained with a goat anti-vimentin antibody (kindly provided by P. Traub, Max Planck Institute for Cell Biology, Ladenburg, Germany) and a secondary, rhodamine-coupled rabbit antigoat antibody (Cappel Laboratories, West Chester, PA). The injected anti-Ct antibody was detected by a secondary, FITC-coupled rabbit antimouse antibody (Zymed Laboratories, San Francisco, CA). Confocal microscopy was performed using a modular confocal microscope, developed and constructed at the EMBL. Double-labeling experiments were performed at an excitation wavelength of 514.5 nm of an Argon-ion laser. Stereo views were generated from confocal image series by pixel shift. For immunoelectron microscopy, the cells, grown on coverslips, were fixed and extracted in the same way as described for immunofluorescence. After incubation with a goat anti-vimentin antibody and washing three times for 10 min with a buffer containing 20 mM Hepes, pH 7.9, 0.25 M KCl, 0.1% fish skin gelatin, and 1% BSA, the cells were incubated with a rabbit antigoat antibody, coupled with 0.8-nm colloidal gold (Aurion GP-ultra small; Aurion, Wageningen, NL). The secondary antibody was added once for 60 min at 37°C, and for a second time overnight. After washing, silver enhancement of the bound gold particles was performed according to Danscher (1981). The cells were stained en bloc with 0.5% uranyl acetate and 1% phosphotungstic acid, dehydrated, and flat-embedded on glass slides in Epon. The glass coverslips were dissolved with HF. Injected cells were selected by phase-contrast light microscopy, cut out of the Epon layer, glued on a preformed Epon block, and sectioned in a ultramicrotome. Ultrathin sections were stained with lead citrate for 1 min, according to Reynolds (1963).

Other Methods

PAGE was performed according to Laemmli (1970). Protein concentrations were measured using a protein determination kit (Bio-Rad Laboratories,

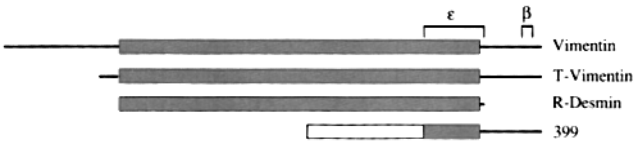

Figure 1. Schematic representation of some IF proteins and fragments used in this study. From top to bottom: intact vimentin (the NH_2-terminal and COOH-terminal nonhelical domains are shown as *bars*, whereas the helical middle domain is shown as a *shaded box*); T-vimentin, a thrombic fragment of vimentin missing its 69 NH_2-terminal residues; R-desmin, a chymotryptic fragment containing the entire helical domain of chicken desmin; 399, a fusion protein containing 99 NH_2-terminal residues of MS2-RNA polymerase (*clear box*) and the 100 COOH-terminal residues of mouse vimentin (*shaded box and bar*). The two epitopes identified by our anti-Ct and anti-anti-Ct (#28) antibodies are shown by ϵ and β, respectively.

Published August 15, 1991

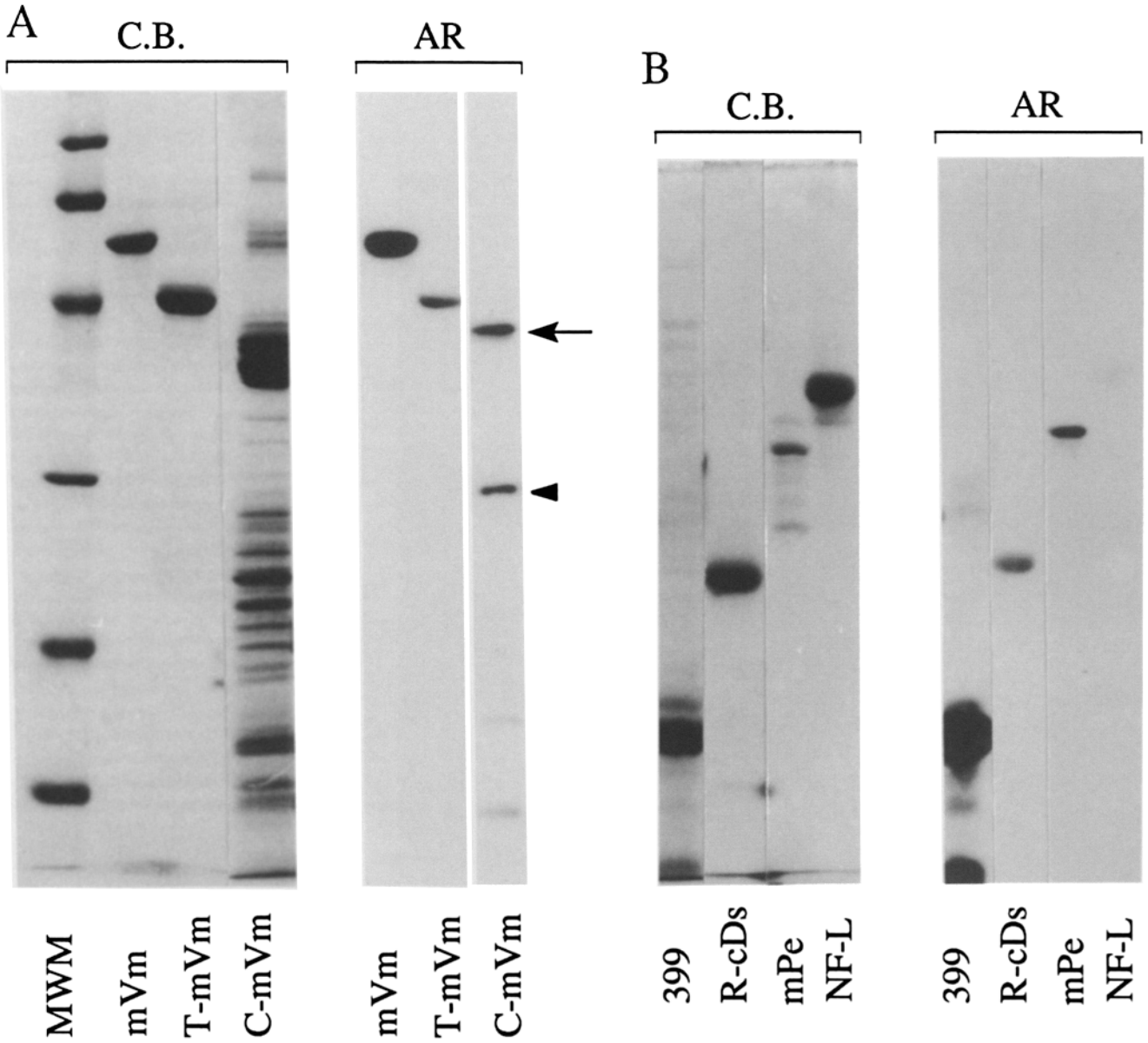

Figure 2. Characterization of the idiotypic, anti-Ct antibodies and identification of the epsilon epitope. (*A* and *B*) Mouse vimentin (*mVm*), thrombin digested mouse vimentin (*T-mVm*), a chymotryptic-digest of mouse vimentin (*C-mVm*), fusion protein 399 (*399*), chicken desmin "rod" fragments (*R-cDs*), mouse peripherin (*mPe*), and porcine 68 kD neurofilament protein (*NF-L*) were electrophoresed in 12% (*A*), or 10% (*B*) SDS-polyacrylamide gels. After electroblotting onto nitrocellulose filters these preparations were probed with 20.0 μg/ml of anti-Ct antibodies and ^{125}I-goat antimouse antibodies. Arrow points to the 38–40-kD "rod" domain of the mouse vimentin preparation and arrowhead to a COOH-terminal subfragment of the "rod" peptide corresponding (in size) to coil 2. C.B. shows Coomassie blue–stained gels and AR autoradiograms of the tested preparations. MWM represents markers with molecular mass values of 97.4, 66.2, 45, 31, 21.5, and 14.4 (in kD).

Palo Alto, CA). Negative staining was done by applying the samples on carbon-coated 300 mesh copper grids (Plano, Marburg, Germany) and staining with 1% uranyl acetate for 1 min at room temperature. Microinjection of 3T3 mouse fibroblast cells with purified anti-Ct IgG (6.5 mg/ml) and anti-IFA (7 mg/ml) was done at room temperature, using a Zeiss automated injection system (Zeiss, Oberkochen, Germany) according to Ansorge and Pepperkok (1988).

Results

Primary Antibodies

In the course of previous experiments, a mAb (anti-Ct) was raised against a fusion peptide containing 100 COOH-terminal residues of mouse vimentin and 99 NH_2-terminal residues of MS2-RNA polymerase (fusion protein 399, containing mouse vimentin residues 364–464; Kouklis, 1990). To localize the epitope of the anti-Ct antibody, we performed immunoblotting analysis on the following preparations: (*a*) intact mouse vimentin; (*b*) T-vimentin (a purified thrombic fragment of vimentin that lacks 70 NH_2-terminal residues); (*c*) a chymotryptic digest of vimentin containing its middle (rod) domain and its COOH-terminal tail domain; (*d*) fusion protein 399; (*e*) R-desmin (a purified chymotryptic fragment of chicken desmin, comprising its entire middle (rod) do-

Published August 15, 1991

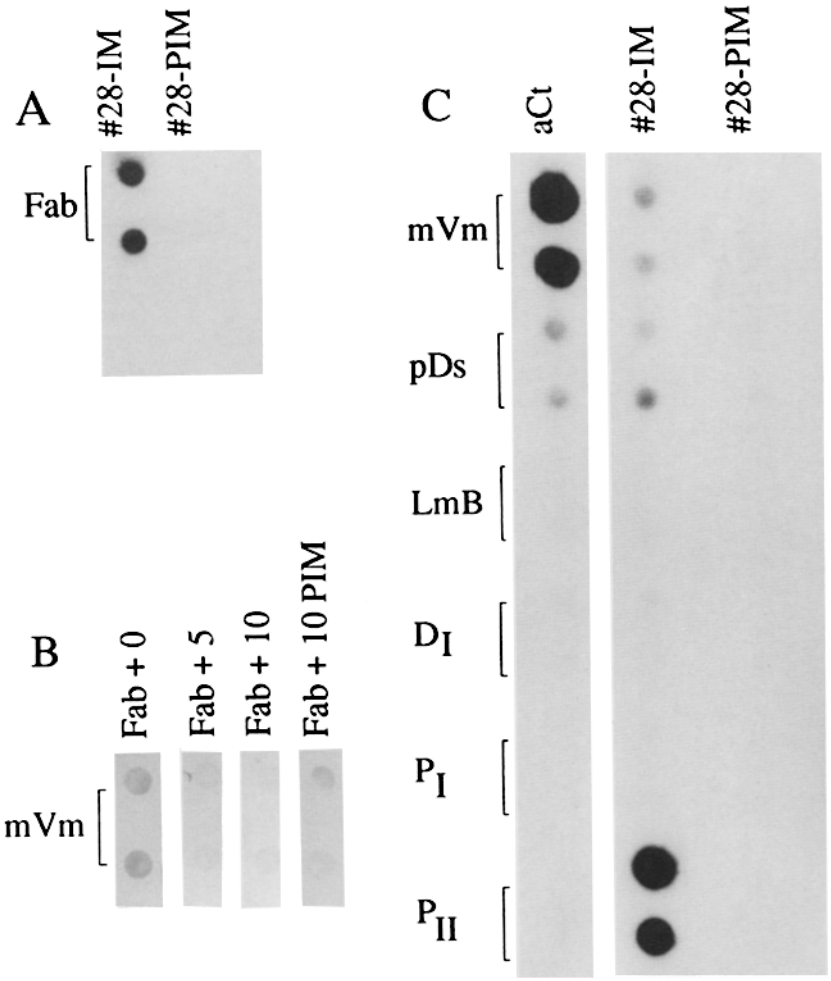

Figure 3. Characterization of the anti-idiotypic antibodies and identification of the beta epitope. (*A*) Anti-Ct Fab fragments (*Fab*) were prepared as described in Materials and Methods. 2.0 μg of this were spotted (in duplicate) onto nitrocellulose filters and probed with either #28 serum (*#28-IM*), or the corresponding preimmune serum (*#28-PIM*), both at a dilution of 1:200. The reaction was developed by ^{125}I-protein A. (*B*) 3.0 μg of purified mouse vimentin (*mVm*) was applied (in duplicate) onto nitrocellulose strips. Replica blots were then probed with 40.0 μg/ml of anti-Ct Fabs mixed with 0.0 μl, 5.0 μl, or 10.0 μl of #28 immune serum (in 2 ml of "gelatin buffer"), or 10.0 μl of preimmune serum, as indicated. The reactions were developed by alkaline phosphatase–conjugated goat antimouse antibodies (light and heavy chain specific). (*C*) ~3.0 μg of mouse vimentin (*mVm*), porcine desmin (*pDs*), rat liver lamin B (*LmB*), and ~28.0 μg of the synthetic peptides DI, PI, and PII (for details see Materials and Methods) were applied (in duplicate) to nitrocellulose filters and probed with #28 immune serum (*#28-IM*), #28 preimmune serum (*#28-PIM*), both diluted 1:150, or with 20.0 μg/ml of anti-Ct antibodies (*aCt*). The reactions were developed with ^{125}I-protein A and ^{125}I-goat antimouse antibodies, respectively.

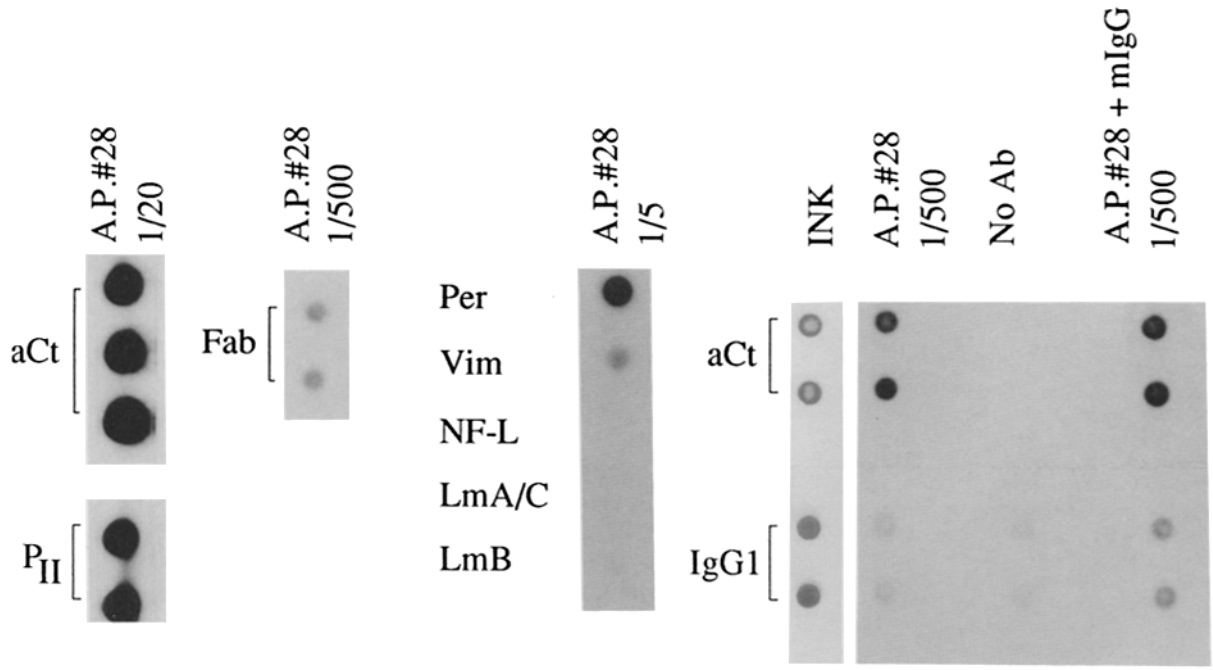

Figure 4. Characterization of the affinity-purified #28 antibodies. #28 immune serum was fractionated by affinity chromatography using affigel 15-PII columns (as specified in Materials and Methods). Antibodies eluted from such columns (diluted as indicated) were then used to probe the following preparations: (*a*) purified anti-Ct IgG (aCt, 2.5, 5.0, and 7.5 μg in the first strip and 3.0 μg in all the other strips); (*b*) anti-Ct Fabs (Fab, 2.0 μg); (*c*) an unrelated mouse IgG1 (IgG1, 3.0 μg); (*d*) PII (PII, 28.0 μg), and (*e*) purified peripherin (*Per*), vimentin (*Vim*), neurofilament L protein (*NF-L*), lamins A/C (*LmA/C*), and lamin B (*LmB*). *A.P. #28 + mIgG* shows an assay done with affinity-purified #28 antibodies (final dilution 1:500) and 50.0 μg/ml of mouse IgG; *No Ab* shows a blot done in the absence of antibodies. All reactions were developed by ^{125}I-protein A. Note the concentration-dependent binding of #28 antibodies to anti-Ct and the background binding of the control IgG1 (partly due to a reaction with ^{125}I-protein A).

Published August 15, 1991

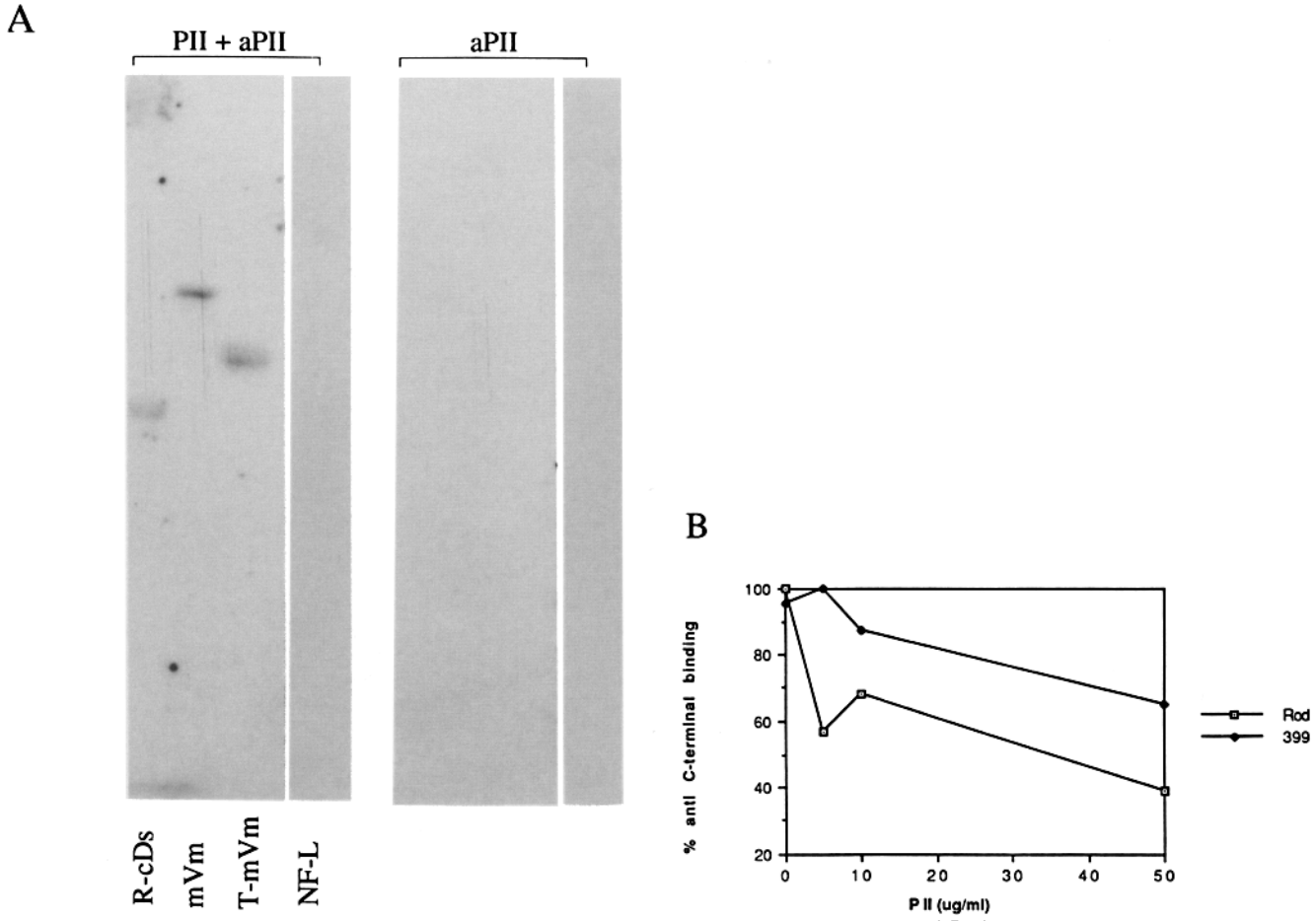

Figure 5. Binding of PII to the epsilon site. (*A*) 2.5 μg of chicken desmin rod fragments (*R-cDs*), mouse vimentin (*mVm*), thrombin-digested mouse vimentin (*T-mVm*), and neurofilament L protein (*NF-L*) were electrophoresed in 10% SDS-polyacrylamide gels. The proteins were transferred to nitrocellulose filters, renatured (Georgatos et al., 1987), and incubated with either 200 μg/ml of PII in "gelatin buffer" (*PII + aPII*), or buffer alone (*aPII*). Binding of PII was detected with a specific antibody against PII (*aPII*; see Djabali et al., 1991) at a dilution of 1:750. The reactions were revealed by ^{125}I-protein A. (*B*) Chicken desmin "rods" (1.3 μg), or fusion protein 399 (2.5 μg) were spotted onto nitrocellulose filters and incubated with 20.0 μg/ml of anti-Ct and increasing concentrations of PII. The reactions were developed by a ^{125}I-goat antimouse antibody, the corresponding spots were cut and their radioactivity was measured in a gamma counter. The plot shows the percentage of antibody binding to the desmin rods and fusion protein 399 as a function of PII concentration. (—⊡—) Rod; (—♦—) 399.

main; (*f*) intact mouse peripherin; and (*g*) intact NF-L. A schematic representation of the main preparations used for antibody mapping is depicted in Fig. 1.

As shown in Fig. 2, *A* and *B* (lanes *mVm*, *T-Vm*, *399*, and *C-mVm*), anti-Ct reacts with intact mouse vimentin, T-vimentin, fusion protein 399, a 38–40-kD chymotryptic peptide corresponding to the rod fragment of vimentin and smaller subfragment of the rod corresponding to coil 2 (Geisler et al., 1982; Quax et al., 1983). The same antibody decorates purified rod fragments of chicken gizzard desmin (Fig. 2 *B*, lane *R-cDs*) (Geisler et al., 1982). Anti-Ct does not recognize the neurofilament L subunit (Fig. 2 *B*, lane *NF-L*) and mammalian lamin B (see below), but gives a positive reaction with mouse peripherin (Fig. 2 *B*, lane *mPe*). These data demonstrate that the anti-Ct epitope occurs in three different type III IF proteins and that it resides in the overlap between the fusion protein 399 and the vimentin rod fragment, i.e., between residues 364 and 416. We have termed this region the "epsilon site or epsilon epitope."

Anti-idiotypic Antibodies

To identify potential epsilon epitope-associating sites along the IF subunit molecules, we immunized rabbits with purified anti-Ct IgG. These sera were then examined for antibodies that have the ability to (*a*) bind to the antigen-binding domain of anti-Ct, i.e., to its Fab fragments; and (*b*) to inhibit binding of anti-Ct Fab fragments to vimentin. As it could be seen in Fig. 3 *A*, the immune serum #28 contains antibodies strongly reacting with anti-Ct Fabs, whereas the corresponding preimmune serum does not give such a reaction. Thus, the anti-anti-Ct activity of the immune serum is the product of a specific immune response and it does not preexist in the serum of the animal before immunization. The anti-idiotypic character of these antibodies can be further confirmed by showing that binding of anti-Ct Fabs to mouse vimentin is inhibited in a concentration-dependent manner by increasing amounts of #28 immune serum (Fig. 3 *B*). The preimmune #28 serum, at the highest concentration, does not affect the

Published August 15, 1991

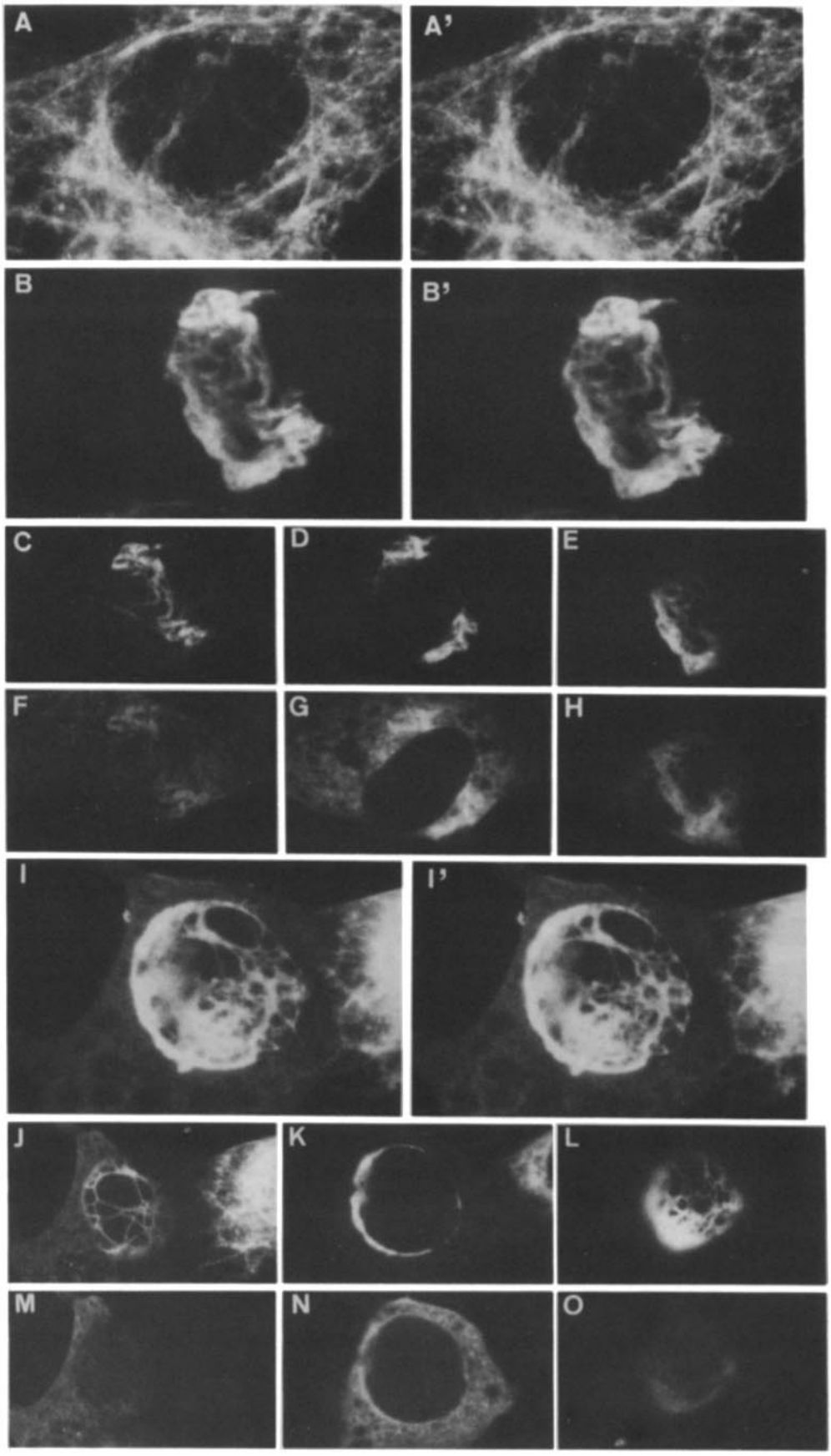

Figure 6. Microinjection experiments and analysis by confocal microscopy. (*A* and *A'*) Stereo pair of the vimentin network in a noninjected 3T3 mouse fibroblast. (*B–H*) A 3T3 mouse fibroblast 3 h after injection of anti-Ct antibody. In *B* and *B'*, a stereo pair of the collapsed vimentin network is shown. *C–E* show the distribution of vimentin at three different focal levels (bottom, middle, top); the location of the injected antibody in the same focal planes is shown in *F–H*. (*I–O*) A specimen 6.5 h after injection of anti-Ct antibody. (*I* and *I'*) Stereo pair of a collapsed vimentin network. (*J–L*) Confocal sections from the bottom (*J*) to the top (*L*) depicting the location of vimentin filaments. *M–O* show the location of the injected antibody. (*P–W*) A specimen 26 h after injection of anti-Ct antibody. (*P* and *P'*) A stereo pair showing the location of vimentin. (*Q–S*) Bottom, middle area, and top of the cell, vimentin staining. (*T–V*) Corresponding images, showing the distribution of the injected antibody. A corresponding image taken in differential interference contrast (*W*) shows the position of the aggregate relative to the nucleus. Magnifications: (*A*, *B*, *I*, and *P*): 1,500×; (*C–H*, *J–O*, *Q–W*) 1,000×.

Published August 15, 1991

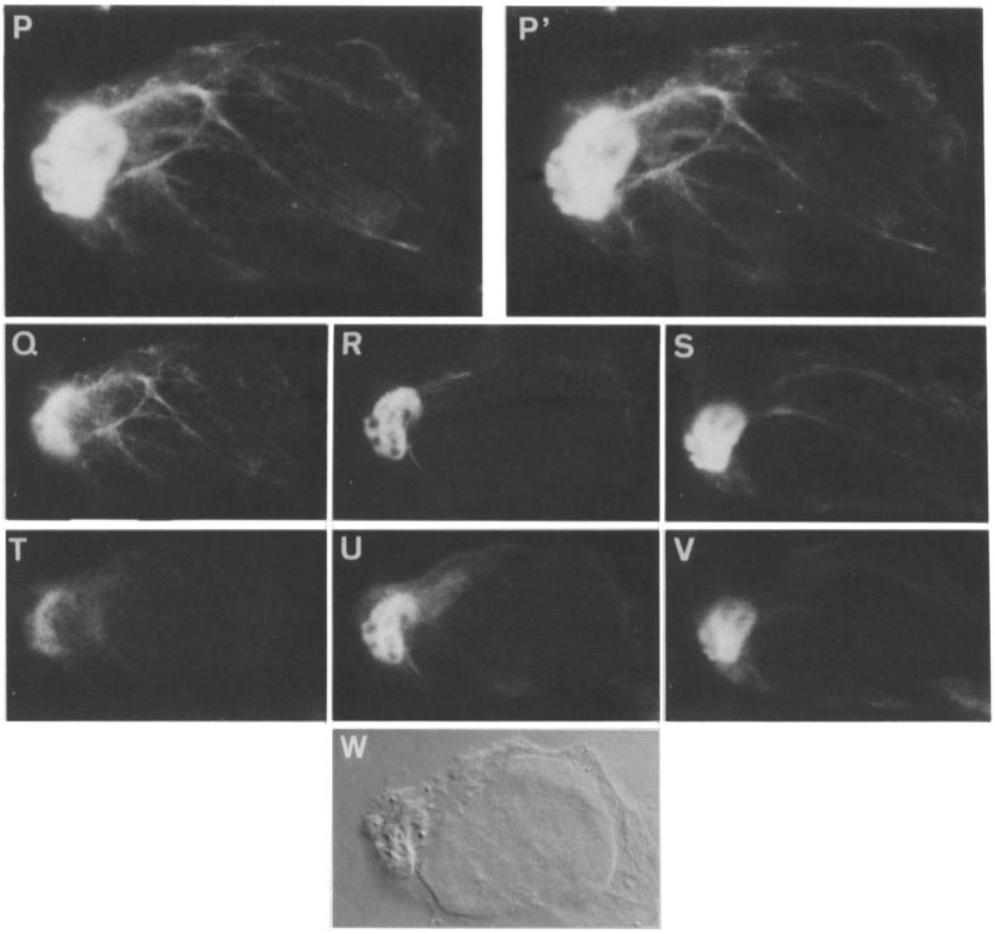

Figure 6.

anti-Ct-vimentin reaction (Fig. 3 *B*). The slight decrease in the signal seen with the preimmune serum is most likely due to a nonspecific effect since this serum does not react with the anti-Ct Fab fragments (see Fig. 3 *A*).

Probing of mouse vimentin, porcine desmin, and rat liver lamin B with the #28 serum reveals a weak, but specific, reaction with the type III IF proteins and a lack of a reaction with lamin B (Fig. 3 *C*, *#28-IM*). The same antibodies react with peripherin, T-vimentin, and fusion protein 399 (data not shown). To map more precisely the #28 antibody epitopes, we tested several peptide preparations, as presented in Fig. 3 *C*. We found that #28 serum gives a strong reaction with a synthetic peptide corresponding to the 30 COOH-terminal residues of mouse neuroblastoma peripherin (PII). Other peptides, representing the proximal 30 residues of the tail domains of mouse neuroblastoma peripherin (PI) and chicken desmin (DI) are not recognized by the #28 antibodies. Hence, the antiserum appears to contain antibodies exclusively addressing a site, common among vimentin, desmin, and peripherin in the region of PII ("beta site or beta epitope"). Inspection of the corresponding sequences (Leonard et al., 1988) reveals, indeed, a highly conserved segment located within 12–20 residues from the COOH-terminal of peripherin, vimentin, and desmin. This sequence (Thr-Ile(Val)-Glu-Thr-Arg-Asp-Gly-X-Val) is absent in non-type III IF proteins, as for example the NF-L subunits or lamin B, and contains a Thr-Arg-Asp-Gly motif that conforms to a "beta-turn."

To rule out cross-reactions due to xenogeneic and allogeneic factors we purified #28 immunoglobulins using a PII-agarose affinity column. Fig. 4 demonstrates that (*a*) the affinity-purified antibodies give a specific and concentration-dependent reaction with anti-Ct IgG and bind to anti-Ct Fabs; (*b*) when anti-Ct IgG and an unrelated mouse IgG1 are probed in parallel with affinity-purified #28 antibodies, only the former give a significant reaction; (*c*) binding of the affinity-purified antibodies to anti-Ct IgG is not inhibited by an excess of mouse IgG; and (*d*) the affinity-purified antibodies react with intact peripherin and vimentin (albeit to a different extent). These results are consistent with the notion that the type III IF proteins react with #28 antibodies via a common site represented in the PII sequence. The difference in the crossreactivity between peripherin and vimentin can be explained by an extra *Lys* residue that occurs in the peripherin molecule and is absent from vimentin (Leonard et al., 1988). These results clearly show that the anti-PII activity contained in the #28 serum represents a genuine anti-idiotypic antibody developed against the paratope of the mAb anti-Ct (Jerne, 1974, 1985).

In Vitro Binding Studies

We reasoned that, if our assumptions are correct, the two

Published August 15, 1991

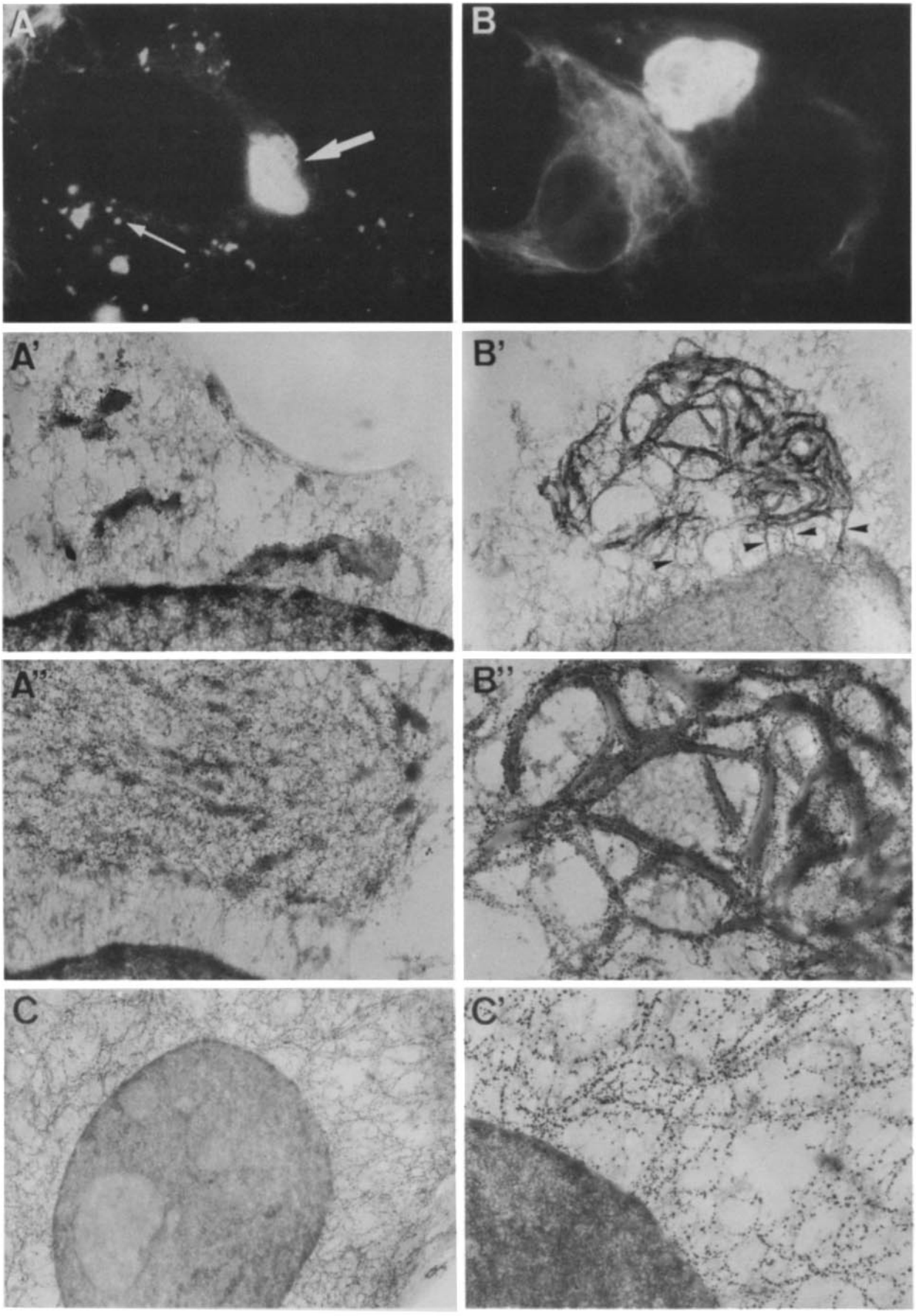

Published August 15, 1991

sites recognized by the idiotypic and anti-idiotypic antibodies (i.e., the epsilon and the beta site) should directly interact with each other. As a consequence, the synthetic peptide PII (that contains the beta site) should be able to associate with intact type III subunits (competing off the intrinsic beta site), or with fragments, such as the rod, or T-vimentin, which contain the epsilon site but lack the rest of the COOH-terminal and the NH_2-terminal domains. Conversely, subunits that do not possess the epsilon site (negative reaction with anti-Ct), as for example the neurofilament L protein, are not expected to bind to PII. The PII peptide should also inhibit binding of anti-Ct to the epsilon epitope.

To test these predictions, intact vimentin, T-vimentin, chicken desmin rods, and neurofilament L subunits were tested using a ligand-blotting assay. As shown in Fig. 5 *A*, PII directly binds to all three type III preparations. However, binding to neurofilament L subunits is not detected. To further confirm that binding of PII occurs at the epsilon epitope, isolated chicken desmin rods and peptide 399 were incubated with a constant amount of anti-Ct and increasing quantities of PII. As shown in Fig. 5 *B*, PII (which is not recognized by anti-Ct antibodies, see Fig. 3 *C*) inhibits binding of anti-Ct to the desmin rod fragments and 399 in a concentration-dependent manner.

Microinjection Experiments and Confocal Microscopy

To examine the potential role of the epsilon-beta interaction in vivo, we microinjected anti-Ct antibodies into vimentin-containing tissue culture cells. Based on the previous in vitro results (Fig. 5), we expected these antibodies to block the epsilon epitope, competing off the beta epitope of vimentin subunits.

Fig. 6, *B–H* show that 3 h after injecting the anti-Ct antibodies into 3T3 cells, IFs lose their radial pattern of distribution and gradually "contract" into thicker fibrils (particularly obvious in Fig. 6 *B*, *B'*, *C*). 6.5 h after injection, confocal microscopy and optical sectioning reveals that the normal *trans*-cytoplasmic IF network has been converted into a cage-like formation in the injected cells. IFs are no longer seen in the periphery of the cells and are concentrated instead in a perinuclear cage made of anastomosed thick fibrils (Fig. 6, *I–O*). Finally, after 1 d, the IFs of injected cells have been converted to a mass with a "reticular" substructure (see below). The position of this mass is not fixed: sometimes the collapsed IFs are seen near the nucleus (Fig. 6, *P–W*), whereas other times they are seen in the cytoplasm and near the plasma membrane (not shown). No filament fragmentation has been observed in the course of such experiments, while the anti-Ct antibodies have always been detected in association with the disorganized IFs. Attempts to repeat the injection experiments with anti-Ct Fab fragments were met with technical difficulties: upon papain fragmentation, the antibodies lost a substantial percentage of their reactivity (consult, for example, Fig. 3 *B*), and upon injection the Fabs remained in the cytoplasm in a diffuse state. To overcome this problem, we employed comparative analysis using other anti-IF antibodies.

Microinjection of 3T3 cells with a mAb against the conserved region of coil 2 (anti-IFA, see Magin et al., 1987; Pruss et al., 1981) produces a different effect. With this antibody, 1 day after injection, the filaments seem to be fragmented into various different masses dispersed in the cytoplasm or being localized near the nucleus (Fig. 7 *A*, *arrows*; a detailed study with these antibodies is to be communicated elsewhere: Kouklis, D.P., Merdes, A., and Georgatos, S.D., manuscript in preparation). Finally, as previously reported (Matteoni and Kreis, 1987), microinjection of 3T3 cells with a third antivimentin mAb (mAb7A3) affects the filaments in yet another manner, producing (predominantly) an asymmetric juxtanuclear "band" or "cap" structure, whereas injection of normal mouse IgG does not alter at all the vimentin filament organization (not shown). These experiments allow us to conclude that the alterations produced by anti-Ct are specific and distinct from those previously seen with other microinjected anti-IF antibodies (for example, see Tölle et al., 1986).

Single-cell Analysis and Immunoelectron Microscopy

Because of the relatively low resolution of optical microscopy, to further examine the specific effect of anti-Ct in vimentin filament organization, cells injected either with anti-Ct, or anti-IFA antibodies were analyzed in parallel by immunoelectron microscopy. By this technique, the various masses produced by anti-IFA injection seem to have an amorphous texture, regardless of their location (Fig. 7, *A'* and *A''*). The mass near the nucleus consists of smaller aggregates, which are interconnected by fine filamentous material (Fig. 7 *A''*). However, in cells injected with the anti-Ct antibody, the mass of aggregated vimentin can be resolved into thick, anastomosed fibrils which are labeled on their surface by a polyclonal antivimentin antibody (Fig. 7 *B''*).

These data, although suggesting a crucial role for the epsilon-beta site interaction in vivo may nevertheless be explained in more than one way ("intercalation" of antibodies between the vimentin subunits at the level of the filament, "systemic" blocking of IF nascent chains and titration of soluble subunits, or interruption of linkages between IFs and other organelles). Therefore, to narrow down these alterna-

Figure 7. Comparison of the effects of microinjected anti-IFA and anti-Ct antibodies by single-cell analysis. (*A–A''*) 3T3 cells were microinjected with anti-IFA (as specified in Materials and Methods). The specimens were fixed after 1 d and analyzed by indirect immunofluorescence (*A*) or immunoelectron microscopy (*A'* and *A''*) using a polyclonal antivimentin antibody. The thin arrow in *A* points to small aggregates dispersed throughout the cytoplasm, which are further resolved by EM in *A'*. The mass of aggregated material (indicated by the *thick arrow* in *A*) is analyzed in *A''*: a fine, immunoreactive meshwork of filaments connects electron dense aggregates. (*B–B''*) Effects of the anti-Ct antibody 1 d after microinjection. In *B* an injected (*right*) and an uninjected (*left*) cell are shown by indirect immunofluorescence. The vimentin filament network in the injected cell is almost completely collapsed into a mass which is further resolved in a similar cell prepared for immunoelectron microscopy (*B'* and *B''*). This mass, which consists of thick anastomosed fibrils (diameter ~100–400 nm), is connected to the nuclear surface by residual vimentin fibers (*arrowheads* in *B'*). A grazing section at the periphery of the nucleus is shown. *B''* is a detail of *B'*. (*C* and *C'*) Uninjected 3T3 cell stained for vimentin. Magnifications: (*A* and *B*) 2,100×; (*B'* and *C*) 3,400×; (*A'*, *A''*, *B''*), (*C'*): 11,000×.

Published August 15, 1991

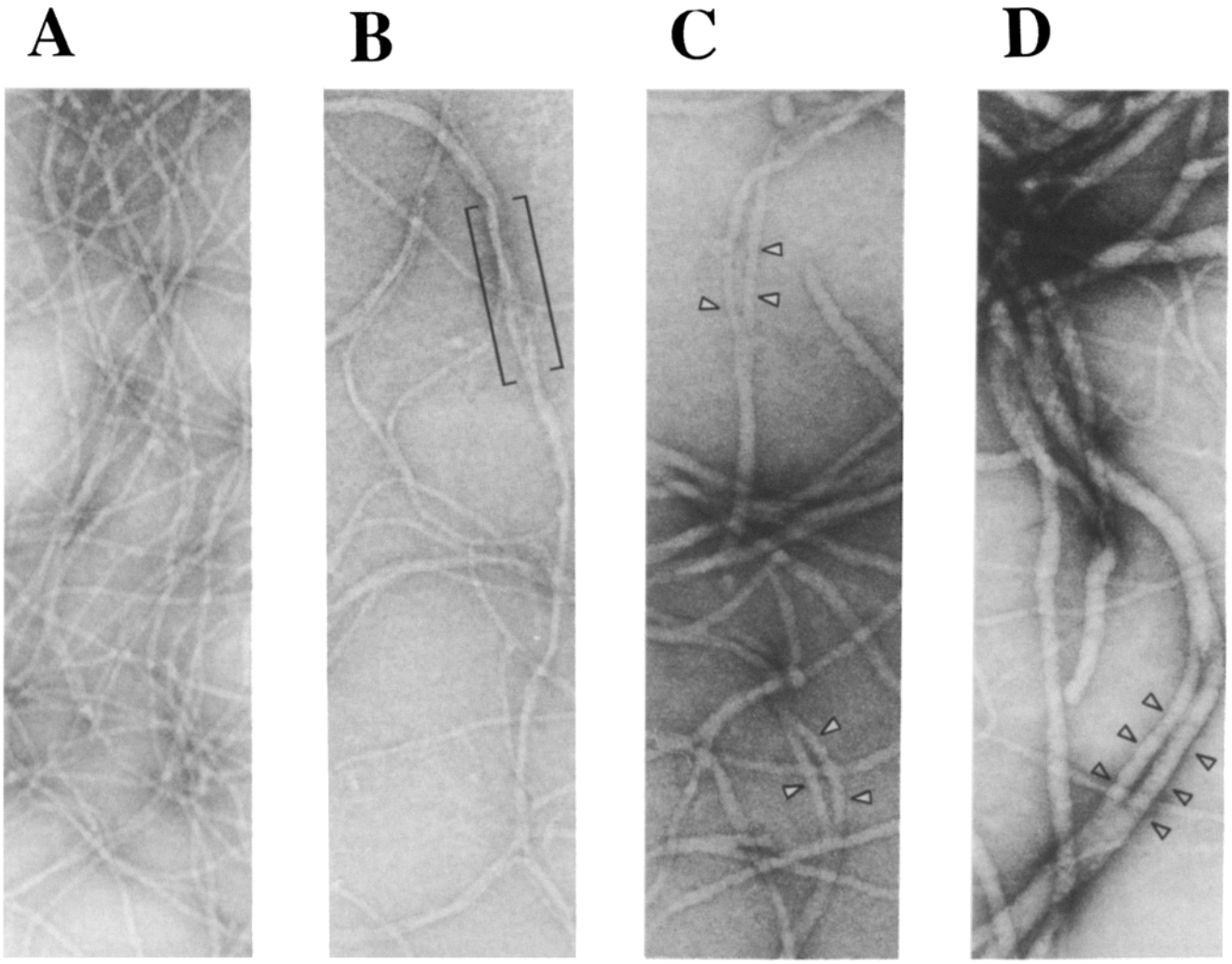

Figure 8. Reconstitution assays. (*A–D*) Purified mouse vimentin protofilaments (400 μg/mi) were mixed with 0 (*A*), 100 (*B*), 500 (*C*) and 1,500 (*D*) μg/ml of PII in 10 mM Tris-HCL, pH 7.4. Samples were preincubated for 60 min at room temperature before addition of concentrated KCl to 150 mM. After an incubation for 60 min at 37°C, the samples were processed for negative staining as specified in Materials and Methods. Note the increase in the diameter of the filaments as the PII concentration is raised. At points, the thick fibrils (diameter ~40–70 nm) seem to divide into subfibers (*brackets* in *B* and *arrowheads* in *C* and *D*). (*E* and *E'*) Vimentin protofilaments at 200 μg/ml were mixed with 1,400 μg/ml of PII and concentrated KCl to a final concentration of 150 mM. The samples were incubated for 30 min at 37°C and then examined by negative staining. *E'* is a higher magnification of an area shown in *E*. (*F*) Vimentin filaments were assembled from protofilamentous material (100 μg/ml) as in *A* above. Such preparations were subsequently incubated with 300 μg/ml of PII for 60 min at 37°C and examined by negative staining. Arrowheads show the periodic decoration of the filament core. (*G* and *H*) Vimentin filaments were assembled as in *A*, absorbed onto microscope grids, and incubated either with assembly buffer (*G*) or with PII (*H*) at a concentration of 500 μg/ml. These specimens were incubated for 120 min with affinity-purified aPII antibodies (Djabali et al., 1991) at a concentration of 50 μg/ml, followed by gold-labeled protein A and finally examined by negative staining. *A–D* and *G–H* are shown in the same magnification. Bars, 100 nm.

tive interpretations and examine the role of the epsilon-beta interaction in filament assembly per se, we carried out reconstitution studies in vitro.

Reconstitution Studies

To induce "uncoupling" of the epsilon from the beta site, a preparation of soluble vimentin protofilaments was preincubated with either buffer, or increasing concentrations of PII, and filament assembly was initiated by addition of salt. Under such conditions (see Fig. 5), the beta site of PII is expected to "titrate" the epsilon site of vimentin subunits, competing off the natural beta site.

At low concentrations of PII, a very slight increase in filament thickness is observed. In all other respects the IFs appear normal (not shown). This precludes stoichiometric "poisoning" and indicates that the epsilon-beta interaction is not involved in filament elongation. However, further increase in the concentration of PII results in filaments with gradually greater diameters, until convoluted thick fibrils (diameter ~40 nm and increasing) dominate the fields (Fig. 8, *B–D*). These thick fibrils are composed of subfibers which, although not immediately obvious, become apparent at points of filament unraveling or branching (Fig. 8, *B–D*, *arrowheads* and *brackets*). In a permutation of the same experiment, PII and salt were added simultaneously to vimentin protofilaments (without a preincubation). Under these conditions, vimentin subunits polymerize and form a network of anastomosed "trabeculae" (Fig. 8 *E*). At high mag-

Published August 15, 1991

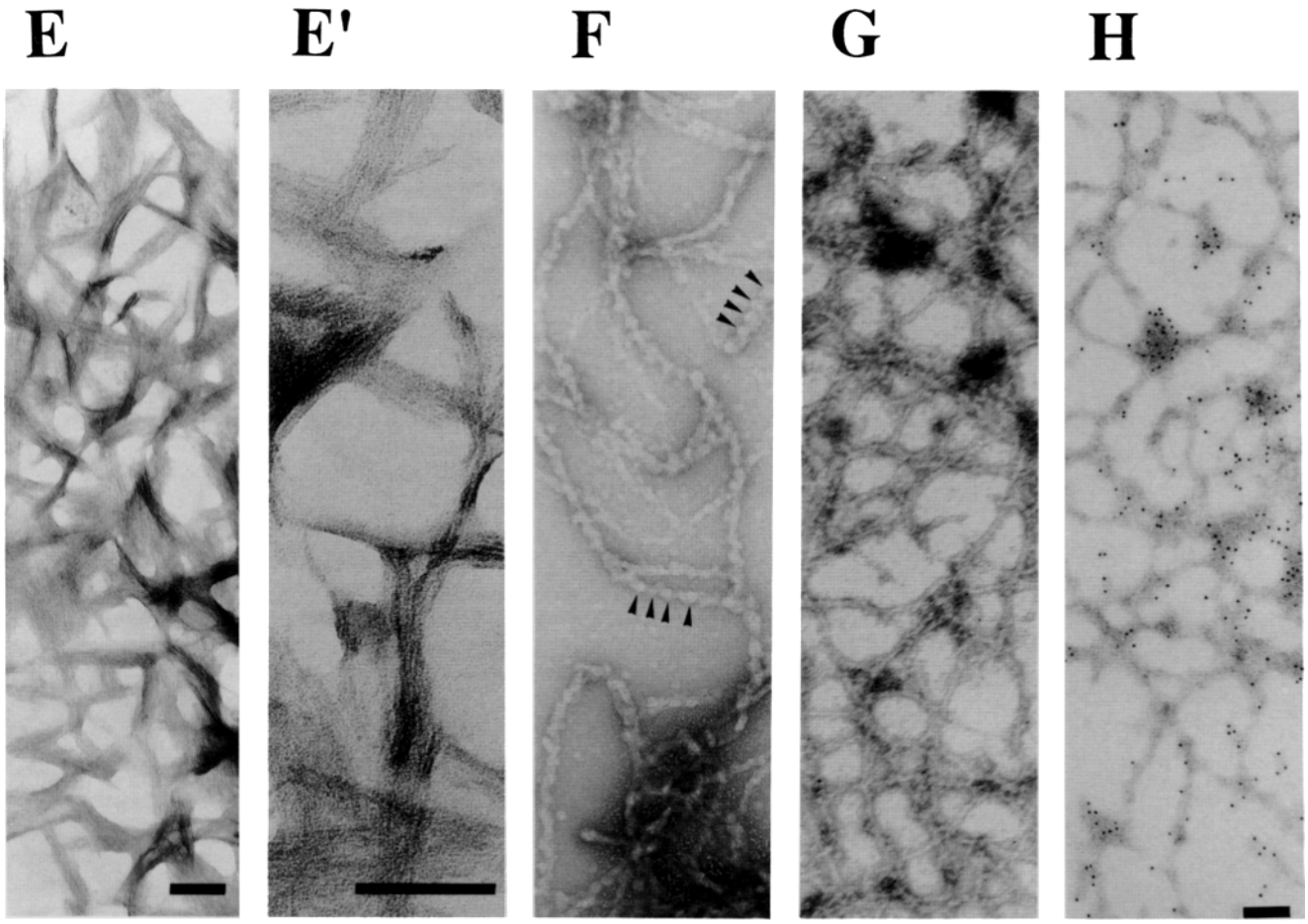

Figure 8.

nification (Fig. 8 *E'*), these structures are seen to contain variable numbers of aligned subfibers. None of these effects were seen using other peptides, modeled after other regions of the type III subunit molecules, while electrophoretic analysis of samples incubated with and without peptides rules out proteolysis in the course of these experiments (P. D. Kouklis and S. D. Georgatos, unpublished observations).

When preassembled vimentin filaments are incubated with PII, a seemingly periodic decoration of the filament backbone is observed (Fig. 8 *F, arrowheads*). The globular particles along the filament core could represent either local "unwinding" of the 10-nm fiber, or sites where PII has bound to IFs. Evidence favoring the second alternative (without excluding the first) is provided by the fact that a specific antibody against PII (aPII) decorates PII-reconstituted vimentin IFs, whereas no decoration is observed when PII is substituted for buffer (Fig. 8, *G* and *H*). These results demonstrate that PII binding to vimentin protofilaments has a pronounced effect on the lateral packing of IFs. However, PII binding to preformed filaments does not seem to change their architecture. Thus, PII seems to exert its effect only when subunits are actively self-associating to form filamentous structures.

In a set of parallel experiments, we also investigated the effect of anti-Ct antibodies on vimentin filament assembly. Fig. 9 (*A* and *A'*) shows that, in the presence of anti-Ct, vimentin forms complex networks composed of anastomosed bundles. The overall morphology of these bundles is virtually identical to the one of the thick fibrils observed after microinjection of the anti-Ct antibodies into 3T3 cells (compare with Fig. 7 *B''*). The effect of anti-Ct on vimentin assembly appears to be very specific and not due to filament cross-linking: out of several antivimentin mAbs that were tested (anti-IFA, mAb 7A3 and other antibodies), anti-Ct has been the only one that produced the filament morphologies described above (data not shown).

Discussion

Network Antibodies as Tools for Studying IF Protein Self-association

We have attempted to study site-specific interactions involving the tail domains of type III IF subunits using network antibodies that replicate complementary features of the associating regions. We have found that anti-idiotypes against a mAb that binds near the end of the helical domain of type III IFs recognize a site located at the COOH-terminal end of the same subunits. Although further refinement of the corresponding epitopes is necessary, the present data provide essentially in vivo evidence for an interaction that involves two different segments of the vimentin molecule, the epsilon and the beta site. Independent binding assays and in vitro reconstitution experiments further support this thesis. Therefore, we propose that network antibodies can be used for studying the self-association of biopolymers.

Published August 15, 1991

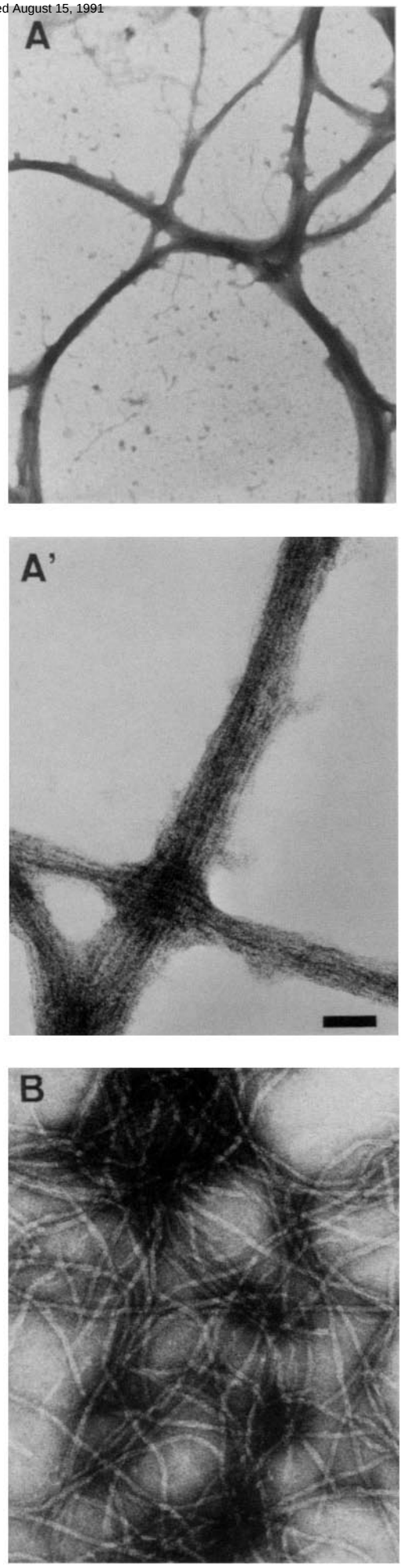

Lateral Organization of Subunit Chains in Type III IFs

Although IF proteins efficiently polymerize into 10-nm filaments in the absence of auxiliary factors (Renner et al., 1981; Zackroff and Goldman, 1979), it remains unknown how the lateral packing of IFs is regulated. Several observations indicate that the thickness of IFs may be subject to some sort of intrinsic control. First, examination of native filaments with scanning-transmission electron microscopy (STEM) reveals significant variations in their mass-per-unit length (Engel et al., 1985; Steven et al., 1982, 1983*a*,*b*). For vimentin, two classes of such polymorphic variants have been detected with a calculated 32 chains and 20–24 chains per filament cross-section, respectively (for a discussion see Steven et al., 1989). Second, in numerous cases, examination of the IFs of tissue-culture cells has also revealed a coexistence of thick filament bundles and dispersed filaments which vary in diameter from 7 to 12 nm. Although IF bundling is thought to be mediated by multivalent cross-linking proteins (Dale et al., 1978), it is also plausible to speculate that the lateral packing of IFs can be regulated by an intrinsic mechanism. From our analysis we would conclude that a site-specific association involving the COOH-terminal domain of type III IFs may provide one of the means for controlling filament thickness and network architecture.

The Role of the Beta–Epsilon Interaction

Our results are most consistent with previous reconstitution experiments showing that desmin subunits missing part of their COOH-terminal domain have a tendency to assemble into bundles or thick, laterally aggregated filaments (Kaufmann et al., 1985; see also Perides et al., 1987). These structures are similar to the thick fibrils and the filament bundles that we have obtained by perturbing the epsilon–beta interaction in vitro or in vivo. Furthermore, nontype III subunits that miss large parts of their COOH-terminal domains, as for example the neurofilament L subunits and the cytokeratins (Gill et al., 1990; Lu and Lane, 1990; Wong and Cleveland, 1990), also show an aberrant assembly behavior under in vivo conditions (although no thick filaments have been observed under these conditions). Interestingly, other IF proteins, as for example the cytokeratins, can apparently assemble in vitro into typical 10-nm filaments, even after removal of their COOH-terminal domains (Hatzfeld and Weber, 1990). However, measurements in cytokeratin filaments assembled from subunits missing part of the tail domain document a noticable trend towards greater filament diameters (Coulombe et al., 1990). It is presently not clear whether such differences are due to subtle solution factors, to differences under in vitro versus in vivo conditions, or to the fact that the COOH-terminal domains of type III proteins have properties distinct from those of the non-type III subunits.

Figure 9. Effect of anti-Ct on vimentin assembly. Vimentin protofilaments at 150 μg/ml were mixed with 1,000 μg/ml of anti-Ct (*A*), or isotonic buffer (*B*) for 60 min at 37°C. After this incubation the salt was adjusted to 150 mM, the specimens were incubated for an additional 60 min at 37°C and finally analyzed by negative staining. *A'* is a higher magnification of *A*. Bar, 100 nm. *B*, same magnification as in *A'*.

Published August 15, 1991

An observation pertinent to our data has recently been published by Birkenberger and Ip (1990). In that case, a synthetic derivative of desmin, representing a segment within the boundaries of the peptide PII, was found to interact with a site of the tail domain of desmin subunits, which is apparently different from the epsilon site. However, because antibodies against this desmin peptide did not cross-react with vimentin subunits, and because the effect of this peptide on desmin filament assembly was clearly different from the one of PII on vimentin filament assembly, it is unlikely that the previous experiments have addressed the same interaction that we have studied.

One interpretation that may explain most of the observations made with type III subunits could be that the interaction between the discontinuous epsilon and beta sites of type III chains results in the formation of a "loop" or "hairpin" structure containing the intervening sequence between these two segments. This loop may include either extented chains, or a relatively compact, globular structure, as in the case of the end domains of the nuclear lamins (Aebi et al., 1986). Such a highly hypothetical arrangement is compatible with the fact that the beta site conforms to a beta-turn (for a pertinent discussion see Djabali et al., 1991). With antiparallel tetramers (Geisler et al., 1985; Stewart et al., 1989), the beta–epsilon interaction is more consistent with an "intramolecular" association. Conversely, if we assume a parallel tetramer (Ip, 1988), the beta–epsilon interaction would involve a dimer-dimer, "intermolecular" association. In any case, surface-exposed loops, formed by adjacent subunits or dimers along the assembled IFs, may prevent the lateral aggregation of neighboring filaments, as previously speculated (Kaufmann et al., 1985). The same structures may limit the lateral growth of individual filaments by sterically shielding subunit addition sites.

The Pivotal Role of Ionic Parameters

That the tendency of truncated desmin subunits to aggregate at physiological salt can be rectified by a simple change of the ionic conditions (Kaufmann et al., 1985) implies that the postulated loops may be covering either similarly charged, or marginally charged "patches" along the IF chains. By removing (or competing off) the part of the COOH-terminal domain which is responsible for loop formation (beta site), these patches could be unmasked or fully neutralized by counterions, allowing for hydrophobically driven subunit–subunit and filament–filament binding. Conversely, lowering the ionic strength may, in turn, strengthen electrostatic repulsion forces or weaken hydrophobic interactions between exposed patches, eliminating any lateral binding. In both cases, the role of ionic factors in normal (10 nm) filament assembly would be rather crucial.

This work is dedicated to Elias Brountzos.

We thank P. Traub and S. Kühn (Max Planck Institute for Cell Biology, Ladenburg, FRG) for providing the anti-Ct antibodies, sharing unpublished data, contributing useful ideas, and commenting on the manuscript. We also thank N. Geisler and K. Weber (Max-Planck Institute for Biophysical Chemistry, Goettingen, FRG) for providing purified chicken desmin rod fragments and NF-L subunits, as well as K. Djabali and G. Simos for useful discussions. The help of W. Ansorge and R. Pepperkok in the microinjection experiments is kindly acknowledged. Finally, we thank B. Sodeik for contributing part of the data shown in Fig. 8.

P. D. Kouklis was supported by a fellowship from the Programme of Cell Biology of EMBL, T. Papamarcaki was supported by a grant from the Greek Ministry of Research and Technology, A. Merdes was supported by a predoctoral fellowship from Studienstiftung des deutschen Volkes.

Received for publication 22 February 1991 and in revised form 13 May 1991.

Note Added in Proof: In a recent report (Shoeman, R. L., E. Mothes, C. Kesselmeier, and P. Traub. 1990. *Cell Biol. International Reports.* 14: 583–594) it has also been observed that vimentin IFs lacking part of their COOH-terminal domain as a result of HIV protease cleavage assemble into "thick" fibers.

References

Aebi, U., J. Cohn, L. Buhle, and L. Gerace. 1986. The nuclear lamina is a meshwork of intermediate-type filaments. *Nature (Lond.).* 323:560–564.

Albers, K., and E. B. Fuchs. 1987. The expression of mutant epidermal keratin cDNAs transfected in simple epithelial and squamus cell carcinoma lines. *J. Cell Biol.* 105:791–806.

Albers, K., and E. B. Fuchs. 1989. Expression of mutant keratin cDNAs in epithelial cells reveals possible mechanisms for initiation and assembly of intermediate filaments. *J. Cell Biol.* 108:1477–1493.

Ansorge, W., and R. Pepperkok. 1988. Performance of an automated system for capillary microinjection into living cells. *J. Biochem. Biophys. Methods.* 16:283–292.

Birkenberger, L., and W. Ip. 1990. Properties of the desmin tail domain: studies using synthetic peptides and antipeptide antibodies. *J. Cell Biol.* 111:2063–2075.

Coulombe, P. A., and E. Fuchs. 1990. Elucidating the early stages of keratin filament assembly. *J. Cell Biol.* 111:153–169.

Coulombe, P. A., Y. Chan, K. Albers, and E. Fuchs. 1990. Deletions in epidermal keratins leading to alterations in filament organization in vivo and in intermediate filament assembly in vitro. *J. Cell Biol.* 111:3049–3064.

Dale, B. A., K. A. Holbrook, and P. M. Steinert. 1978. Assembly of stratum corneum basic protein and keratin filaments in macrofibrils. *Nature (Lond.).* 276:729–731.

Danscher, G. 1981. Histochemical demonstration of heavy metals. A revised version of the sulfide silver method suitable for both light and electron microscopy. *Histochemistry.* 71:1–16.

Djabali, K., M. M. Portier, F. Gros, G. Blobel, and S. D. Georgatos. 1991. Network antibodies identify nuclear lamin B as a physiological attachment site for peripherin intermediate filaments. *Cell.* 64:109–121.

Engel, A., R. Eichner, and U. Aebi. 1985. Polymorphism of reconstituted human epidermal keratin filaments: determination of their mass-per-length and width by scanning transmission electron microscopy. *J. Ultrastruct. Res.* 90:323–335.

Geisler, N., and K. Weber. 1982. The amino acid sequence of chicken muscle desmin provides a common structural model for intermediate filaments. *EMBO (Eur. Mol. Biol. Organ.) J.* 1:1649–1656.

Geisler, N., E. Kaufmann, and K. Weber. 1982. Proteinchemical characterization of three structurally distinct domains along the protofilament unit of desmin 10 nm filaments. *Cell.* 30:277–286.

Geisler, N., E. Kaufmann, S. Fischer, U. Plessmann, and K. Weber. 1983. Neurofilament architecture combines structural principles of intermediate filaments with carboxy-terminal extensions increasing in size between triplet proteins. *EMBO (Eur. Mol. Biol. Organ.) J.* 2:1295–1300.

Geisler, N., E. Kaufmann, and K. Weber. 1985. Antiparallel orientation of the double-stranded coiled-coils in the tetrameric protofilament unit of intermediate filaments. *J. Mol. Biol.* 182:173–177.

Georgatos, S. D., and G. Blobel. 1987*a*. Two distinct attachment sites for vimentin along the plasma membrane and the nuclear envelope in avian erythrocytes: a basis for a vectorial assembly of intermediate filaments. *J. Cell Biol.* 105:105–115.

Georgatos, S. D., and G. Blobel. 1987*b*. Lamin B constitutes an intermediate filament attachment site at the nuclear envelope. *J. Cell Biol.* 105:117–125.

Georgatos, S. D., K. Weber, N. Geisler, and G. Blobel. 1987. Binding of two desmin derivatives to the plasma membrane and the nuclear envelope of avian erythrocytes: evidence for a conserved site-specificity in intermediate filament-membrane interactions. *Proc. Natl. Acad. Sci. USA.* 84:6780–6784.

Gill, S. R., P. C. Wong, M. J. Monteiro, and D. W. Cleveland. 1990. Assembly properties of dominant and recessive mutations in the small mouse neurofilament (NF-L) subunit. *J. Cell Biol.* 111:2005–2019.

Hatzfeld, M., and K. Weber. 1990. Tailess keratins assemble into intermediate filaments in vitro. *J. Cell Sci.* 97:317–324.

Hanukoglu, I, and E. B. Fuchs. 1983. The cDNA sequence of type II cytoskeletal keratin reveals constant and variable structural domains among keratins. *Cell.* 33:915–924.

Hennekes, H. 1990. Clonierung und Charakterisierung des Mousgens für das Intermediärfilamentprotein Vimentin. Ph.D. thesis. University of Hannover, FRG. 126 pp.

Hisanaga, S., and N. Hirokawa. 1988. Structure of the peripheral domains of

neurofilaments revealed by low angle rotary shadowing. *J. Mol. Biol.* 202:297–305.

Hoger, T., G. Krohne, and W. W. Franke. 1988. Amino acid sequence and molecular characterization of murine lamin B as deduced from cDNA clones. *Eur. J. Cell Biol.* 47:283–290.

Ip, W. 1988. Modulation of desmin intermediate filament assembly by a monoclonal antibody. *J. Cell Biol.* 106:735–745.

Jerne, N. K. 1974. Towards a network theory of the immune system. *Ann. Immunol. (Inst. Pasteur).* 125:C:373–389.

Jerne, N. K. 1985. The generative grammar of the immune system. *EMBO (Eur. Mol. Biol. Organ.) J.* 4:847–852.

Kaufmann, E., K. Weber, and N. Geisler. 1985. Intermediate forming ability of desmin lacking either the amino-terminal 67 or the carboxy-terminal 27 residues. *J. Mol. Biol.* 185:733–742.

Kouklis, P. 1990. Herstellung, Charakterisierung und Anwendung Monoklonaler Antikörper gegen Maus-Vimentin. Ph.D. thesis. University of Heidelberg, FRG. 107 pp.

Laemmli, U. K. 1970. Cleavage of structural proteins during the assembly of the head of bacteriophage T4. *Nature (Lond.).* 227:680–685.

Landon, F., M. Lemonnier, R. Benarous, C. Huc, M. Fiszman, F. Gros, and M. -M. Portier. 1989. Multiple mRNAs encode peripherin, a neuronal intermediate filament protein. *EMBO (Eur. Mol. Biol. Organ.) J.* 8:1719–1726.

Lazarides, E. 1980. Intermediate filaments as mechanical integrators of cellular space. *Nature (Lond.).* 283:249–256.

Leonard, D. G. B., J. D. Gorham, P. Cole, L. A. Greene, and E. D. Ziff. 1988. A nerve growth factor-regulated messenger RNA encodes a new intermediate filament protein. *J. Cell Biol.* 106:181–193.

Lu, X., and E. B. Lane. 1990. Retrovirus-mediated transgenic keratin expression in cultured fibroblasts: specific domain functions in keratin stabilization and filament formation. *Cell.* 62:681–696.

Magin, T. M., M. Hatzfeld, and W. W. Franke. 1987. Analysis of cytokeratin domains by cloning and expression of intact and deleted polypeptides in Escherichia coli. *EMBO (Eur. Mol. Biol. Organ.) J.* 6:2607–2615.

Matteoni, R., and T. E. Kreis. 1987. Translocation and clustering of endosomes and lysosomes depends on microtubules. *J. Cell Biol.* 105:1253–1265.

Nelson, W. J., and P. Traub. 1982. Purification and further characterization of the Ca^{2+}-activated proteinase specific for the intermediate filament proteins vimentin and desmin. *J. Biol. Chem.* 257:5536–5543.

Pain, D., H. Murakami, and G. Blobel. 1990. Identification of a receptor for protein import into mitochondria. *Nature (Lond.).* 347:444–449.

Perides, G., S. Kühn, A. Scherbarth, and P. Traub. 1987. Probing of the structural ability of vimentin and desmin-type intermediate filaments with Ca^{2+}-activated proteinase, thrombin and lysin-specific endoproteinase. *Eur. J. Cell Biol.* 43:450–458.

Pruss, R. M., R. Mirsky, M. C. Raff, R. Thorpe, A. J. Dowding, and B. H. Anderton. 1981. All class of intermediate filaments share a common antigenic determinant defined by a monoclonal antibody. *Cell.* 27:419–428.

Quax, W., W. V. Egberts, W. Hendriks, Y. Quax-Jeuken, and H. Bloemendal. 1983. The structure of the vimentin gene. *Cell.* 35:215–223.

Quax, W., L. Van de Brock, W. V. Egberts, F. Ramaekers, and H. Bloemendal. 1985. Characterization of the hamster desmin gene: expression and formation of desmin filaments in nonmuscle cells after gene transfer. *Cell.* 43:327–338.

Renner, W., W. W. Franke, N. Schmid, K. Weber, and E. Mandelkow. 1981. Reconstitution of intermediate-sized filaments from denatured monomeric vimentin. *J. Mol. Biol.* 149:285–306.

Reynolds, E. S. 1963. The use of lead citrate at a high pH as an electron opaque stain in electron microscopy. *J. Cell Biol.* 17:208–212.

Rivas, C. I., J. C. Vera, and R. B. Maccioni. 1988. Anti-idiotypic antibodies that react with microtubule-associated proteins are present in sera of rabbits immunized with synthetic peptides from tubulin's regulatory domain. *Proc. Natl. Acad. Sci. USA.* 85:6092–6096.

Shechter, Y., R. Maron, D. Elias, and I. R. Cohen. 1982. Autoantibodies to insulin receptor spontaneously develop as anti-idiotypes in mice immunized with insulin. *Science (Wash. DC).* 216:542–545.

Shechter, Y., D. Elias, R. Maron, and I. R. Cohen. 1984. Mouse antibodies to the insulin receptor developing spontaneously as anti-idiotypes. *J. Biol. Chem.* 259:6411–6415.

Steinert, P. M., and D. R. Roop. 1988. Molecular and cellular biology of intermediate filaments. *Annu. Rev. Biochem.* 57:593–625.

Steinert, P. M., R. H. Rice, D. R. Roop, B. L. Trus, and A. C. Steven. 1983. Complete amino acid sequence of a mouse epidermal keratin subunit and implications for the structure of the intermediate filaments. *Nature (Lond.).* 302:794–800.

Steven, A. C., J. S. Wall, J. T. Hainfeld, and P. M. Steinert. 1982. Structure of fibroblastic intermediate filaments: analysis by scanning transmission electron microscopy. *Proc. Natl. Acad. Sci. USA.* 79:3101–3105.

Steven, A. C., J. F. Hainfeld, B. L. Trus, J. S. Wall, and P. M. Steinert. 1983*a*. The distribution of mass in heteropolymer intermediate filaments assembled in vitro. *J. Biol. Chem.* 258:8323–8329.

Steven, A. C., J. F. Hainfeld, B. L. Trus, J. S. Wall, and P. M. Steinert. 1983*b*. Epidermal keratin filaments assembled in vitro have masses-per-unit-length that scale according to average subunit masses: structural basis for homologous packing of subunits in intermediate filaments. *J. Cell Biol.* 97:1939–1944.

Steven, A. C., J. W. Mack, B. L. Trus, M. E. Bisher, and P. M. Steinert. 1989. Structural and assembly of intermediate filaments: multi-faceted, myosin-like (but non-motile) cytoskeletal polymers. Cytoskeletal and extracellular proteins. U. Aebi and J. Engel, editors. Springer-Verlag, FRG. 15–26.

Stewart, M., R. A. Quinlan, and R. D. Moir. 1989. Molecular interactions in the paracrystals of a fragment corresponding to the helical coiled-coil rod portion of glial fibrillar acidic protein: evidence for an antiparallel packing of molecules and polymorphism related to intermediate filament structure. *J. Cell Biol.* 109:225–234.

Tolle, H. -G., K. Weber, and M. Osborn. 1986. Microinjection of monoclonal antibodies to vimentin, desmin, and GFAP in cells which contain more than one IF type. *Exp. Cell Res.* 162:462–474.

Traub, P., and C. E. Vorgias. 1983. Involvement of the N-terminal polypeptide of vimentin in the formation of intermediate filaments. *J. Cell Sci.* 63:43–67.

Vaux, D., J. Tooze, and S. Fuller. 1990. Identification by anti-idiotype antibodies of an intracellular membrane protein that recognizes a mammalian endoplasmic reticulum retention signal. *Nature (Lond.).* 345:495–502.

Wong, P. C., and D. W. Cleveland. 1990. Characterization of dominant and recessive assembly-defective mutations in mouse neurofilament NF-M. *J. Cell Biol.* 111:1987–2003.

Zackroff, R. V., and R. D. Goldman. 1979. In vitro assembly of intermediate-sized filaments from baby hamster kidney (BHK-21) cells. *Proc. Natl. Acad. Sci. USA.* 76:6226–6230.

Zehner, Z. E., Y. Li, B. A. Roe, B. M. Paterson, and C. M. Sax. 1987. The chicken vimentin gene: nucleotide sequence, regulatory elements, and comparison to the hamster gene. *J. Biol. Chem.* 262:8112–8120.